The release of catanionic mixtures embedded in gels: An approximate analytical analysis

Göran Frenning[1], Johan Gråsjö and Per Hansson

Department of Pharmacy, Uppsala University, P.O. Box 580, SE-751 23 Uppsala, Sweden

This is a reprint of work published in AIChE J 57, 1402–1408, 2011

http://dx.doi.org/10.1002/aic.12368

We present an approximate analytical analysis of the release of catanionic mixtures from gels. The starting points are the monomer–mixed micelle equilibrium, described by using regular solution theory, and the one-dimensional diffusion equation. Focusing on a half-infinite planar system, we first point out an exact reduction of the problem to a system of ordinary differential equations. By using the pseudo-steady-state approximation and the integral-balance method, we then derive a single nonlinear equation for the mole fraction of drug in micelles at the extraction front. This equation may be readily solved numerically (or graphically), and once the solution is found, all quantities of interest may be determined in closed form. Comparisons with numerical solutions of the fully nonlinear problem indicate that the errors resulting from the approximations typically do not exceed 10 %.

Keywords: Controlled drug delivery, release; Drug release; Mathematical modeling; Diffusion; Catanionic mixtures

[1]Corresponding author

Email: goran.frenning@farmaci.uu.se, Fax: +46 18-471 42 23, Phone: +46 18-471 43 75

Introduction

Catanionic mixtures have been suggested as a rather generic means of prolonging the release of drugs from gels.[1–3] The basic idea is to take advantage of the major characteristics of such mixtures, namely the large size of the mixed aggregates and the low concentration of free amphiphiles in equilibrium with the aggregates. Large aggregates, such as vesicles or wormlike micelles, are expected to be effectively immobilized inside a gel matrix. Under such conditions the release is governed solely by the diffusive transport of single molecules, a slow process when the concentration of dispersed monomers is low. The concept has been demonstrated for catanionic mixtures of amphiphilic drugs and regular surfactants at physiological salt concentration;[1–5] the release rate from gels has been found to be 10–100 times lower than in control experiments without surfactant. In combination with the other advantages of gels as pharmaceutical dosage forms, e.g., mucoadhesiveness and injectability, the systems are interesting for drug delivery.

Mixed micelles of surfactants have been studied extensively both from a fundamental view point (see Refs. 6 and 7 and references therein) and as candidate systems for drug delivery.[8] The micellar morphology depends on the nature as well as on the mole fraction of the mixed surfactants, and can often be rationalized using the concepts of packing parameter or spontaneous curvature. Catanionic mixtures typically form bilayers when the surfactants are present in equal proportions,[9] a behavior reflecting the close packing of the head groups possible in this case. Vesicles are often formed in dilute dispersions of such mixtures.[10–13] However, with increasing mole fraction of either surfactant, transitions to, in turn, wormlike and globular micelles occur,[14–20] a natural progression considering the expected increase of aggregate curvature with increasing surface charge density. A general property of mixed micellar systems, due to entropy of mixing, is that the equilibrium concentration of free monomers is lower than the pure

component critical micelle concentration (CMC). For the component present at a mole fraction < 0.5 in catanionic aggregates, the effect is strongly reinforced by the electrostatic interactions, leading to free concentrations several orders of magnitude below the CMC. Furthermore, the CMC of the mixture is considerably lower than the CMC of either component for a wide range of compositions, a synergy effect due to, chiefly, that the entropic penalty for micelle formation from counterion binding is removed when the components neutralize each other.[7] In the regular solution approach to mixed micelles,[21] the non-ideal effects are collected in one interaction parameter (β). Despite its simplicity, the model is quite efficient in describing variations of the free concentrations, even for catanionic mixtures,[22,23] but in the latter case only when salt is present in excess. At low ionic strength, more detailed models are required to handle properly the electrostatic effects.[6,7,24–26] Many amphiphilic drugs lack the typical head-and-tail structure of surfactants and form micelles with low aggregation numbers (if at all). Nevertheless, mixtures of amphiphilic drugs and oppositely charged surfactants can display properties typical of catanionic mixtures, including aggregate morphology and variation of the mixed CMC with total composition, as has been demonstrated earlier.[2,4,5]

Recently, a detailed model for the release of catanionic mixtures from gels was proposed,[23] which was based on regular solution theory.[21] The underlying assumption was that surfactants (charged drug and counter ions) in stationary aggregates were in equilibrium with mobile monomers, which were gradually released by diffusion. The aggregates will henceforth be referred to as 'micelles', although they often take the form of vesicles or wormlike micelles, as discussed above. As a result mainly of the highly nonlinear equilibrium conditions, a numerical solution of the governing equations was required. Since the need for a numerical solution of partial differential equations (PDEs) may limit the applicability of an otherwise relatively straightforward theory, the purpose of this work is to devise a much simpler solution procedure. To this end, we investigate a half-infinite planar system (rather than a system of finite extent).

For this particular geometry, one finds an exact reduction of the problem to a system of ordinary differential equations (ODEs). To derive an approximate analytic solution is nevertheless not a trivial task. In this work, we use a combination of the pseudo-steady-state approximation and the integral-balance method. Comparisons are made with numerical solutions of the fully nonlinear problem.

Theory

Model formulation

As already indicated, we consider a half-infinite planar system, occupying the spatial region $x > 0$. The system contains two oppositely charged surfactants that form mixed micelles when their total concentration exceeds the mixed CMC, as determined from regular solution theory.[21] We let $C_i(x,t)$ and $S_i(x,t)$ be the monomer and micelle concentration of component i (= 1 or 2), respectively, which are functions of the spatial coordinate x and time t, as indicated. Above the mixed CMC, regular solution theory states that[21]

$$C_1 = X e^{\beta(1-X)^2} \mathrm{CMC}_1 \ , \tag{1}$$

$$C_2 = (1-X) e^{\beta X^2} \mathrm{CMC}_2 \ , \tag{2}$$

where $X = S_1/(S_1 + S_2)$ is the mole fraction of component 1 in micelles. In these expressions, CMC_i is the CMC of component i and β is an interaction parameter. Introducing the total micelle concentration $M = S_1 + S_2$, one may express the component micelle concentrations as

$$S_1 = XM \ , \tag{3}$$

$$S_2 = (1-X)M \tag{4}$$

above the mixed CMC.

When transport occurs via monomer diffusion only, mass conservation of each component may be expressed by Fick's second law,[23]

$$D_i \frac{\partial^2 C_i}{\partial x^2} = \frac{\partial C_i}{\partial t} + \frac{\partial S_i}{\partial t} \ , \tag{5}$$

where D_i is the diffusion coefficient of component i. To simplify the analysis, we assume that the gel initially contains a uniform amount of both components and that sink conditions are enforced on the boundary at $x = 0$. The relevant boundary conditions thus are

$$C_i(0, t) = 0 \ , \tag{6}$$

$$\lim_{x \to \infty} C_i(x, t) = C_{i0} \ , \tag{7}$$

whereas the initial conditions take the form

$$C_i(x, 0) = C_{i0} \ . \tag{8}$$

In these expressions, C_{i0} is the initial monomer concentration of component i, in equilibrium with the micelle concentration S_{i0}, as calculated from regular solution theory. The initial surfactant concentration is assumed to exceed the mixed CMC, so that micelles exist in the system.

Model reduction

For the assumed half-infinite system, the Boltzmann transformation,[27]

$$\eta = \frac{x}{2\sqrt{t}} \ , \tag{9}$$

reduces the PDEs (5) to ODEs in the reduced variable η. The transformed equations read

$$D_i \ddot{C}_i + 2\eta \left(\dot{C}_i + \dot{S}_i \right) = 0 \ , \tag{10}$$

where the superposed dots denote differentiation with respect to η. Moreover, the *combined* initial and boundary conditions may be expressed as

$$C_i(0) = 0 \,, \tag{11}$$

$$\lim_{\eta\to\infty} C_i(\eta) = C_{i0} \,. \tag{12}$$

When micelles are present in the system initially, an extraction front will develop with time, separating an outer depletion region without micelles from an inner region where micelles coexist with monomers, as found in Ref. 23. The location of this front will be denoted by η_* in the reduced description. The spatial location of the front thus increases with the square-root of time, $x_* = 2\eta_*\sqrt{t}$, in accordance with the observations made in Ref. 23.

Balance equations

It is clear the monomer concentrations must be continuous across the extraction front, which we indicate by writing $C_i^{*+} = C_i^{*-}$, where the asterisks denote values at η_* and the plus and minus signs are used to distinguish between values immediately above and below the front. Integrating Eq. (10) across the front, noting that $S_i^{*-} = 0$ by definition, one finds that

$$D_i \left(\dot{C}_i^{*+} - \dot{C}_i^{*-} \right) + 2\eta_* S_i^{*+} = 0 \,. \tag{13}$$

Similarly, integrating Eq. (10) over the entire inner region, excluding the front, one obtains the equation

$$\begin{aligned} &D_i \dot{C}_i^{*+} + 2\eta_* \left(\Delta C_i^{*+} + \Delta S_i^{*+} \right) \\ &\quad + \int_{\eta_{*+}}^{\infty} 2(\Delta C_i + \Delta S_i) \, \mathrm{d}\eta = 0 \,, \end{aligned} \tag{14}$$

where integration by parts has been performed and where the primitive functions to $\dot{C}_i$ and $\dot{S}_i$ have been written as $\Delta C_i = C_i - C_{i0}$ and $\Delta S_i = S_i - S_{i0}$ to ensure that the generalized integral remains finite. Equations (13) and (14) may be used as starting points for the derivation of an approximate solution.

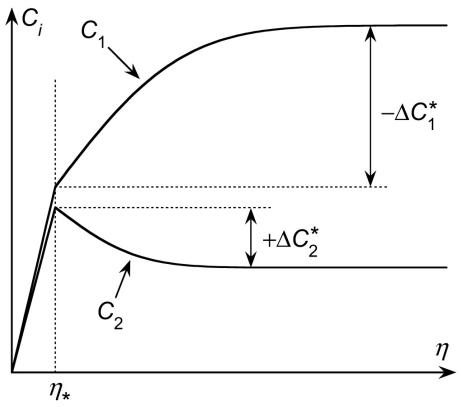

Figure 1: Schematic illustration of the monomer concentration profiles used in the approximate analysis.

Approximate analytical analysis

Provided that the micelle concentrations are sufficiently large, one may use the pseudo-steady-state approximation[28] in the outer region, implying that the monomer concentrations increase linearly with η, so that

$$\dot{C}_i^{*-} \approx \frac{C_i^{*+}}{\eta_*} \,, \tag{15}$$

where we have utilized the fact that the monomer concentrations are continuous across the front at η_*. The pseudo-steady-state approximation is expected to be valid provided that the ratio between the total concentration $T_{i0} = C_{i0} + S_{i0}$ and the monomer concentration C_{i0} is larger than about 3.[29]

We use the (heat) integral-balance method, originally proposed by Goodman,[30] in the inner region. To this end, we postulate error-function variations of the monomer and micelle concentrations,

$$\Delta C_i \approx \Delta C_i^{*+} \operatorname{erfc}[\kappa_i(\eta - \eta_*)] \,, \tag{16}$$

$$\Delta S_i \approx \Delta S_i^{*+} \operatorname{erfc}[\kappa_i(\eta - \eta_*)] \,, \tag{17}$$

where $\operatorname{erfc}(\cdot)$ is the complementary error function[31] and κ_i are as yet unspecified constants.

The above functional forms are motivated by the fact that the approximate first-order solutions, obtained by linearizing the governing equations, would be of the error-function type (see Supplementary Material). It is however not straightforward to a priori determine how well the approximate concentration profiles (16) and (17) describe the actual situation in the nonlinear regime. For this reason, we have resorted to comparisons with the numerical solution of the fully nonlinear problem (see below). A schematic illustration of the monomer concentration profiles is provided in Fig. 1.

The derivative of the Ansatz (16) with respect to η equals $-2\kappa_i \Delta C_i^* / \sqrt{\pi}$ immediately above the front, and since this derivative shall equal $\dot{C}_i^{*+}$, one obtains

$$\kappa_i = -\frac{\sqrt{\pi}\dot{C}_i^{*+}}{2\Delta C_i^{*+}} \, . \tag{18}$$

When the approximate variations in monomer and micelle concentrations expressed by Eqs. (16) and (17) are used, one may evaluate the integral in Eq. (14) as

$$\begin{aligned} \int_{\eta_{*+}}^{\infty} 2(\Delta C_i + \Delta S_i) \, \mathrm{d}\eta &\approx \frac{2(\Delta C_i^{*+} + \Delta S_i^{*+})}{\sqrt{\pi}\kappa_i} \\ &= -\frac{4(\Delta C_i^{*+} + \Delta S_i^{*+})\Delta C_i^{*+}}{\pi \dot{C}_i^{*+}} \, , \end{aligned} \tag{19}$$

where Eq. (18) has been used in the last step.

Using the approximation (15) in Eq. (13), utilizing Eqs. (1)–(4) to give the result a more explicit form, one obtains

$$D_1 \left(\eta C_1' \dot{X} - C_1 \right) + 2\eta^2 X M = 0 \, , \tag{20}$$

$$D_2 \left(\eta C_2' \dot{X} - C_2 \right) + 2\eta^2 (1 - X) M = 0 \, , \tag{21}$$

where the prime denotes differentiation with respect to X and the sub- and superscripted asterisks and pluses have been dropped since all variables are to be evaluated immediately

above the front at η_*. Similarly, use of the approximation (19) in Eq. (14) results in

$$\pi D_1(C_1'\dot{X})^2 + [2\pi\eta C_1'\dot{X} + 4(C_{10} - C_1)]$$
$$\times [C_1 - T_{10} + XM] = 0 \,, \tag{22}$$
$$\pi D_2(C_2'\dot{X})^2 + [2\pi\eta C_2'\dot{X} + 4(C_{20} - C_2)]$$
$$\times [C_2 - T_{20} + (1 - X)M] = 0 \,. \tag{23}$$

Noting that C_1' and C_2' are known functions of X as a result of the equilibrium conditions (1) and (2), Eqs. (20)–(23) may be seen as a nonlinear equation system in the four unknowns η, M, X and $\dot{X}$.

Eliminating $\dot{X}$ between Eqs. (20) and (21), one obtains an equation of the form

$$\eta^2 M U_2 + U_1 = 0 \,, \tag{24}$$

where U_1 and U_2 are functions of X only (explicit forms are provided in the appendix). By using Eq. (20) to eliminate $\dot{X}$ from Eq. (22), one finds that

$$\eta^4 M V_4 + \eta^2 M V_3 + \eta^2 V_2 + V_1 = 0 \,, \tag{25}$$

where V_1, V_2, V_3 and V_4 all are functions of X only (with explicit forms again given in the appendix). Similarly, use of Eq. (21) to eliminate $\dot{X}$ from Eq. (23) produces

$$\eta^4 M W_4 + \eta^2 M W_3 + \eta^2 W_2 + W_1 = 0 \,, \tag{26}$$

where W_1, W_2, W_3 and W_4 again all are functions of X only (refer to the appendix).

Equations (24) and (25) may be readily solved for M and η^2 [Eq. (24) shows that $\eta^2 M = -U_1/U_2$, and this relation reduces Eq. (25) to a linear equation in η^2]. The result may be expressed as

$$\eta^2 = -\frac{H_1}{H_2} \,, \tag{27}$$
$$M = \frac{U_1 H_2}{U_2 H_1} \,, \tag{28}$$

where

$$H_1 = U_1 V_3 - U_2 V_1 \ , \tag{29}$$

$$H_2 = U_1 V_4 - U_2 V_2 \ . \tag{30}$$

Finally inserting the values for η^2 and M provided by Eqs. (27) and (28) in Eq. (26), one finds that

$$F = H_1 H_4 - H_2 H_3 = 0 \ , \tag{31}$$

where the first equality defines a function $F(X)$ and where we have let

$$H_3 = U_1 W_3 - U_2 W_1 \ , \tag{32}$$

$$H_4 = U_1 W_4 - U_2 W_2 \ . \tag{33}$$

Equation (31) provides a nonlinear equation for X that may readily be solved numerically or graphically. Some care must be exercised, however, because the equation $F(X) = 0$ generally has more than one root for X between zero and one. This does not pose any serious problems in practice, as the following discussion demonstrates.

If each component would behave independently, no changes in monomer or micelle concentrations would occur in the inner region, and different front positions would in general be obtained for each component. When the steady-state-approximation is used, it is straightforward to deduce from Eq. (13) that the front position for component i then would be

$$\eta_{*i} = \sqrt{\frac{D_i C_{i0}}{2 S_{i0}}} \ . \tag{34}$$

The mixed-micelle system will compensate so that a single front position η_* is obtained, and η_* will therefore lie between η_{*1} and η_{*2}. This knowledge may be utilized in the following manner: If η_{*1} is *less* than η_{*2}, the monomer concentration C_1 has to increase from its equilibrium value C_{10}. Since C_1 always is an increasing function of X, this in turn implies that the mole fraction X

has to increase from its equilibrium value X_0, and we may therefore select the first root *greater* than X_0. If, on the other hand, η_{*1} is *greater* than than η_{*2}, the monomer concentration and the mole fraction both have to decrease, and the first root *less* than X_0 is to be selected. In the exceptional case that η_{*1} and η_{*2} coincide, the common value is the correct front position and no changes in mole fraction or concentrations occur in the inner region.

Once the front position and the mole fraction at the front have been obtained, the release rate may be readily determined by noting that the outward flux has magnitude

$$J_i = D_i \frac{\partial C_i}{\partial x}\bigg|_{x=0} = \frac{D_i \dot{C}_i(0)}{2\sqrt{t}} \approx \frac{D_i C_i^*}{2\eta_* \sqrt{t}} \,, \tag{35}$$

where the final expression is a consequence of the pseudo-steady-state approximation, Eq. (15). The amount released per unit area may thus be expressed as

$$Q_i = D_i \dot{C}_i(0) \sqrt{t} \approx \frac{D_i C_i^*}{\eta_*} \sqrt{t} = K_i \sqrt{t} \,, \tag{36}$$

where the last equality defines a rate constant K_i.

Numerical analysis

The numerical solution to the fully nonlinear problem may most conveniently be determined by using a shooting procedure. A nonlinear ODE system in $X(\eta)$ and $M(\eta)$ is obtained when the expressions (1)–(4) for the monomer and micelle concentrations in the inner region are inserted in Eq. (10). This ODE system is second order in X and first order in M, and the specification of X, $\dot{X}$ and M at η_* hence produces a unique solution that allows values of X and M at large η to be determined. Since no micelles exist in the outer region, the exact solutions to Eq. (10) may in this region be expressed as

$$C_i = A_i \operatorname{erf}\left(\eta / \sqrt{D_i}\right) \,, \tag{37}$$

where $\operatorname{erf}(\cdot)$ is the error function[31] and A_i are integration constants. When the solutions (37) are inserted in the matching conditions (13), and the continuity requirements on the monomer

Table 1: Parameter values used in the first stage of the evaluation of the analytical approximation (from Ref. 23).

	D (cm^2/s)	CMC (mM)	$\beta_{\mathrm{drug/SDS}}$ ($-$)
Diph	4.8×10^{-6}	105	-8.4
Tet	4.8×10^{-6}	75	-9.0
SDS	4.8×10^{-6}	1.2	–

concentrations are taken into account, it is found that $\dot{X}_* = \dot{X}(\eta_*)$ and $M_* = M(\eta_*)$ may be expressed as functions of η_* and $X_* = X(\eta_*)$. The overall solution procedure thus amounts to (i) assigning values to η_* and X_*, (ii) calculating $\dot{X}_*$ and M_* using the derived closed-form expressions, (iii) numerically solving the ODE system with X_*, $\dot{X}_*$ and M_* as boundary conditions at η_*, to obtain $X_\infty = \lim_{\eta\to\infty} X(\eta)$ and $M_\infty = \lim_{\eta\to\infty} M(\eta)$ and (iv) adjusting η_* and X_* until X_∞ and M_∞ coincide with the target values X_0 and $M_0 = S_{10} + S_{20}$.

Comparison with numerical data

The derived approximate analytic solutions were validated in two stages. In the first, they were compared to initial release rates extracted from literature data pertaining to a slab geometry.[23] In the second, extensive numerical calculations were performed for the half-infinite geometry investigated in this work.

Focusing first on the slab geometry, we thus consider the same systems as in Ref. 23, i.e., catanionic mixtures of sodium lauryl sulfate (SDS) and either of two drugs, the antihistamine diphenhydramine (Diph) and the local anesthetic tetracaine (Tet). In total, four compositions were investigated (values indicate total concentrations in mM): Diph/SDS 14/26, Diph/SDS

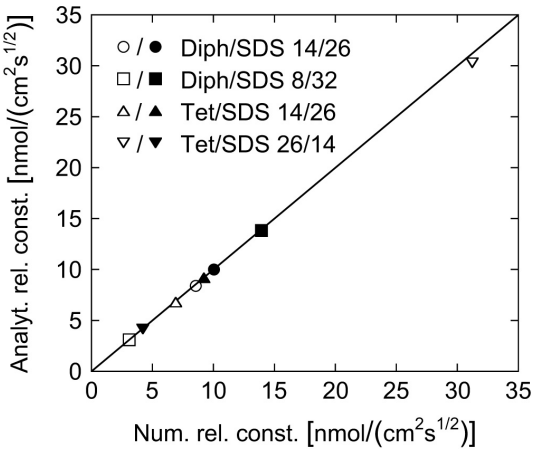

Figure 2: Comparison between numerically and analytically determined release constants K_i [cf. Eq. (36)] for the slab geometry.

8/32, Tet/SDS 14/26 and Tet/SDS 26/14. For the readers convenience, parameter values used in the analysis are summarized in Table 1.

In Fig. 2, the approximate analytically determined release constants K_i [cf. Eq. (36)] are displayed as a function of the numerically determined ones, based on release data presented in Ref. 23. Although systems of finite size were investigated in the mentioned reference, all release profiles were linear when displayed as a function of $\sqrt{t}$ during the first hour of the release process, enabling accurate determinations of the release constants from the numerical data.

As may be seen, there is a good agreement between analytical and numerical results, with an error generally not exceeding a few percent. The worst agreement is observed for the Tet/SDS 26/14 system, for which the approximate analysis underestimates the release of Tet by about 3 %. The Tet/SDS 26/14 system is exceptional in the sense that the Tet monomer concentration decreases considerably in the inner region, from a value of about 7.8 mM for large η to a value of approximately 1.2 mM at the front (as obtained from the numerical solution). Considering that a calculation of release rates based on equilibrium values would have overestimated the release rate for Tet by more than a factor of 6, the approximate result is considered quite satisfactory

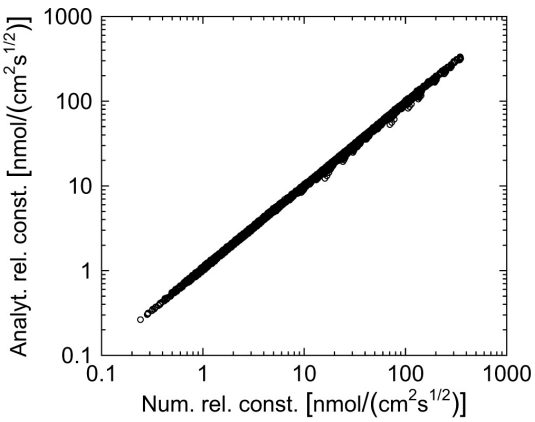

Figure 3: Comparison between numerically and analytically determined release constants for the half-infinite geometry.

also in this case.

Having established that the approximate analytic solutions are valid for the literature data, we next turn our attention to the half-infinite geometry. Numerical and analytical model calculations were performed for 3 levels of the interaction parameter β (-15, -10 and -5), diffusion coefficients D_1 and D_2 (5, 10 and 15×10^{-6} cm^2/s) and CMC's (1, 10 and 100 mM) and 4 levels of the total concentrations T_{10} and T_{20} (10, 40, 70 and 100 mM). For each substance and level of β, there are $n = 3 \times 3 \times 4 = 36$ combinations of diffusion coefficients, CMC's and total concentrations. Excluding degenerate systems, for which there effectively is only one substance present, this results in $N = n(n-1)/2 = 630$ unique combinations for each level of β. The total number of systems considered is thus $3N = 1890$, but no micelles were obtained for $\beta = -5$, $\mathrm{CMC}_1 = \mathrm{CMC}_2 = 100$ mM and $T_{10} = T_{20} = 10$ mM, reducing this number by 3 (since there are 3 unique combinations of nonequal diffusion coefficients). The total data set thus consisted of $2 \times (3N - 3) = 3774$ values, since two release constants were determined for each system.

This data set is illustrated in Fig. 3, which displays the approximate analytically determined release constants as a function of the numerically determined ones on a doubly logarithmic

scale. There is overall a good agreement between the analytical and numerical results, but some deviations may also be seen. In particular, the release rate is underestimated by the analytical solution for some parameter values, most likely as a result of the pseudo-steady-state assumption. If one insists that the pseudo-steady-state conditions be fulfilled in the sense that the ratios C_{10}/T_{10} and C_{20}/T_{20} both are smaller than 1/3, the maximal relative error of the analytically determined release constants is 14 % compared to 25 % for the entire data set. The calculations also indicate that inaccuracies may sometimes result if the monomer concentrations are very small; if one demands that the ratios C_{10}/T_{10} and C_{20}/T_{20} also be larger than 2×10^{-4}, the maximal relative error is reduced to 10 %.

Conclusions

By using the pseudo-steady-state approximation and the integral-balance method, an approximate analytical solution was derived for the release of catanionic mixtures from gels. The analytical solution was found to be of sufficient accuracy to be practically useful, as indicated by comparison with the numerical solution of the fully nonlinear problem, and is straightforward to apply.

Acknowledgments

Financial support to this investigation provided by the Swedish Research Council (Project No. 621-2007-3854) is gratefully acknowledged.

Literature cited

1. Paulsson M, Edsman K. Controlled drug release from gels using surfactant aggregates. II. Vesicles formed from mixtures of amphiphilic drugs and oppositely charged surfactants.

Pharm Res. 2001;18:1586–1592.

2. Bramer T, Paulsson M, Edwards K, Edsman K. Catanionic Drug–Surfactant Mixtures: Phase Behavior and Sustained Release from Gels. *Pharm Res*. 2003;20:1661–1667.

3. Bramer T, Dew N, Edsman K. Catanionic mixtures involving a drug: A rather general concept that can be utilized for prolonged drug release from gels. *J Pharm Sci*. 2006; 95:769–780.

4. Bramer T, Dew N, Edsman K. Pharmaceutical applications for catanionic mixtures. *J Pharm Pharmacol*. 2007;59:1319–1334.

5. Dew N, Bramer T, Edsman K. Catanionic mixtures formed from drugs and lauric or capric acid enable prolonged release from gels. *J Colloid Interface Sci*. 2008;323:386–394.

6. Nagarajan R. Molecular theory for mixed micelles. *Langmuir*. 1985;1:331–341.

7. Shiloach A, Blankschtein D. Predicting micellar solution properties of binary surfactant mixtures. *Langmuir*. 1998;14:1618–1636.

8. Lasic DD. Mixed micelles in drug delivery. *Nature*. 1992;355:279–280.

9. Jokela P, Jönsson B, Khan A. Phase equilibria of catanionic surfactant–water systems. *J Phys Chem*. 1987;91:3291–3298.

10. Kaler EW, Murthy AK, Rodriguez BE, Zasadzinski JAN. Spontaneous vesicle formation in aqueous mixtures of single-tailed surfactants. *Science*. 1989;245:1371–1374.

11. Marques EF, Regev O, Khan A, Miguel MdG, Lindman B. Vesicle Formation and general phase behavior in the catanionic mixture SDS–DDAB–water. The anionic-rich side. *J Phys Chem B*. 1998;102:6746–6758.

12. Marques EF, Regev O, Khan A, Miguel MdG, Lindman B. Vesicle formation and general phase behavior in the catanionic mixture SDS–DDAB–water. The cationic-rich side. *J Phys Chem B*. 1999;103:8353–8363.

13. Tondre C, Caillet C. Properties of the amphiphilic films in mixed cationic/anionic vesicles: a comprehensive view from a literature analysis. *Adv Colloid Interface Sci*. 2001;93:115–134.

14. Bergström LM, Bastardo LA, Garamus VM. A small-angle neutron and static light scattering study of micelles formed in aqueous mixtures of a nonionic alkylglucoside and an anionic surfactant. *J Phys Chem B*. 2005;109:12387–12393.

15. Hassan PA, Narayanan J, Manohar C. Vesicles and worm-like micelles: Structure, dynamics and transformations. *Current Science*. 2001;80:980–989.

16. Lin Z. Branched worm-like micelles and their networks. *Langmuir*. 1996;12:1729–1737.

17. Raghavan SR, Fritz G, Kaler EW. Wormlike micelles formed by synergistic self-assembly in mixtures of anionic and cationic surfactants. *Langmuir*. 2002;18:3797–3803.

18. Rodriguez C, Acharya DP, Maestro A, Hattori K, Aramaki K, Kunieda H. Effect of nonionic head group size on the formation of worm-like micelles in mixed nonionic/cationic surfactant aqueous systems. *J Chem Eng Jpn*. 2004;37:622–629.

19. Schubert BA, Kaler EW, Wagner NJ. The microstructure and rheology of mixed cationic/anionic wormlike micelles. *Langmuir*. 2003;19:4079–4089.

20. Varade D, Ushiyama K, Shrestha LK, Aramaki K. Wormlike micelles in Tween-80/C_mEO_3 mixed nonionic surfactant systems in aqueous media. *J Colloid Interface Sci*. 2007;312:489–497.

21. Holland PM, Rubingh DN. Nonideal multicomponent mixed micelle model. *J Phys Chem.* 1983;87:1984–1990.

22. Holland PM, Rubingh DN. Cationic surfactants in mixed surfactant systems. In: *Cationic Surfactants*, edited by Holland PM, Rubingh DN, vol. 37 of *Surfactant Science Series 37*, pp. 141–187. New York: Marcel Decker. 1991;.

23. Bramer T, Frenning G, Gråsjö J, Edsman K, Hansson P. Implications of regular solution theory on the release mechanism of catanionic mixtures from gels. *Colloids Surf B.* 2009; 71:214–225.

24. Bergström LM, Bramer T. Synergistic effects in mixtures of oppositely charged surfactants as calculated from the Poisson-Boltzmann theory: A comparison between theoretical predictions and experiments. *J Colloid Interface Sci.* 2008;322:589–595.

25. Jönsson B, Wennerström H. Phase equilibria in a three-component water–soap–alcohol system. A thermodynamic model. *J Phys Chem.* 1987;91:338–352.

26. Hansson P, Jönsson B, Ström C, Söderman O. Determination of micellar aggregation numbers in dilute systems with the fluorescence quenching method. *J Phys Chem B.* 2000; 104:3496–3506.

27. Crank J. *The mathematics of diffusion.* Oxford: Oxford University Press, 2nd ed. 1979.

28. Higuchi T. Rate of release of medicaments from ointment bases containing drugs in suspension. *J Pharm Sci.* 1961;50:874–875.

29. Higuchi T. Mechanisms of sustained action medication: Theoretical analysis of the rate of release of solid drugs dispersed in solid matrices. *J Pharm Sci.* 1963;52:1145–1149.

30. Goodman TR. The heat-balance integral and its application to problems involving a change of phase. *Trans ASME.* 1958;80:335–342.

31. Abramowitz M, Stegun IA, eds. *Handbook of mathematical functions.* New York: Dover Publications, Inc. 1965.

Appendix: Explicit expressions for coefficients

This appendix provides explicit expressions for the coefficients U_i, V_j and W_j ($i = 1, 2$ and $j = 1, \ldots, 4$). Specifically, the coefficients U_i in Eq. (24) may be expressed as

$$U_1 = C_1 C_2' - C_2 C_1' \,, \tag{38}$$

$$U_2 = 2\left[\frac{(1-X)C_1'}{D_2} - \frac{XC_2'}{D_1}\right] \,. \tag{39}$$

The coefficients V_j in Eq. (25) take the form

$$V_1 = \pi C_1^2 \,, \tag{40}$$

$$V_2 = -\frac{2(T_{10} - C_1)(\pi C_1 - 2C_1 + 2C_{10})}{D_1} \,, \tag{41}$$

$$V_3 = -\frac{2X[\pi C_1 + 2(C_1 - C_{10})]}{D_1} \,, \tag{42}$$

$$V_4 = \frac{4\pi X(T_{10} - C_1)}{D_1^2} \,. \tag{43}$$

Finally, the coefficients W_j in Eq. (26) are

$$W_1 = \pi C_2^2 \,, \tag{44}$$

$$W_2 = -\frac{2(T_{20} - C_2)(\pi C_2 - 2C_2 + 2C_{20})}{D_2} \,, \tag{45}$$

$$W_3 = -\frac{2(1-X)[\pi C_2 + 2(C_2 - C_{20})]}{D_2} \,, \tag{46}$$

$$W_4 = \frac{4\pi(1-X)(T_{20} - C_2)}{D_2^2} \,. \tag{47}$$

As might be anticipated, the coefficients W_j are obtained from the coefficients V_j by substituting $1 - X = X_2$ for $X = X_1$ and C_2 for C_1, etcetera.